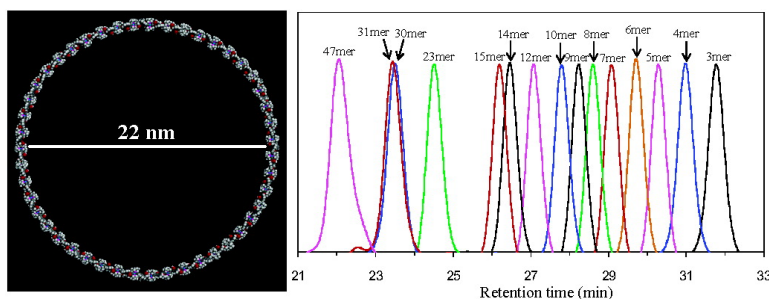


Expeditious Assembly of Mesoscopic Metalloclusters

Hua Jiang, and Wenbin Lin

J. Am. Chem. Soc., **2004**, 126 (24), 7426-7427 • DOI: 10.1021/ja049145m • Publication Date (Web): 27 May 2004

Downloaded from <http://pubs.acs.org> on March 31, 2009



More About This Article

Additional resources and features associated with this article are available within the HTML version:

- Supporting Information
- Links to the 3 articles that cite this article, as of the time of this article download
- Access to high resolution figures
- Links to articles and content related to this article
- Copyright permission to reproduce figures and/or text from this article

[View the Full Text HTML](#)

Expedient Assembly of Mesoscopic Metallopolycycles

Hua Jiang and Wenbin Lin*

Department of Chemistry, CB #3290, University of North Carolina, Chapel Hill, North Carolina 27599

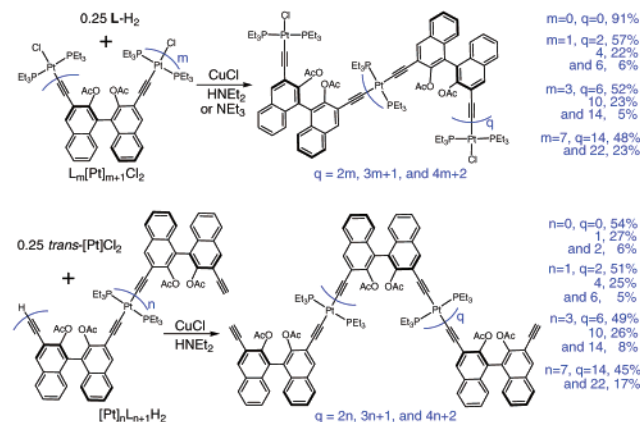
Received February 16, 2004; Revised Manuscript Received May 4, 2004; E-mail: wlin@unc.edu

The synthesis of polygonal structures via coordination-driven self-assembly processes has witnessed tremendous growth in the past decade.¹ Although numerous metallopolycycles of triangular and square topologies have been reported,² larger molecular polygons are much more difficult to obtain because of their entropic disadvantage.¹ We recently reported efficient self-assembly of chiral metallopolycycles ranging from triangle to octagon by taking advantage of kinetic inertness of the Pt-alkynyl linkage.³ This method is, however, not amenable to the synthesis of even larger molecular polygons. Herein we wish to report expeditious stepwise directed-assembly of chiral metallopolycycles containing as many as 47 metal centers by cyclization of metal- and ligand-terminated oligomers under kinetic control. These unprecedented mesoscopic molecular polygons are built from 2,2'-diacetoxy-1,1'-binaphthyl-3,3'-bis(ethyne) (**L-H**₂) bridging ligand and *trans*-Pt(PEt₃)₂ (**[Pt]**) metal connector, and they exhibit interesting size-exclusion behavior.

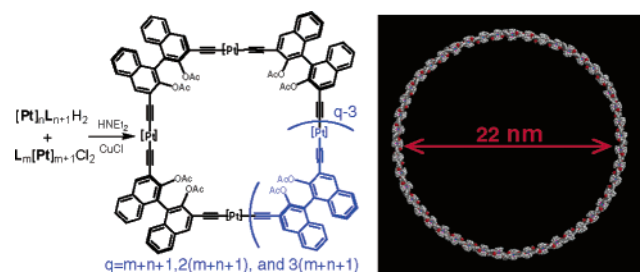
The requisite metal- and ligand-terminated oligomers were synthesized via an iterative process as shown in Scheme 1.⁴ For example, treatment of **L**[**Pt**]₂Cl₂ with 0.25 equiv of **L-H**₂ at room temperature (r.t.) yielded metal-terminated oligomers **L**_{*m*}[**Pt**]_{*m*+1}-Cl₂ in 85% overall yield, and each of them was purified by column chromatography (*m* = 3, 57%; *m* = 5, 22%; and *m* = 7, 6%).⁵ Reaction of **L**₇[**Pt**]₈Cl₂ and 0.25 equiv of **L-H**₂ at r.t. led to even longer **L**_{*m*}[**Pt**]_{*m*+1}Cl₂ oligomers (*m* = 15, 48% and *m* = 23, 23%). Ligand-terminated oligomers **[Pt]**_{*n*}**L**_{*n*+1}H₂ (*n* = 1, 3, 5, 7, 10, 15, and 23) were similarly obtained by using excess **L-H**₂ in the iterative assembly processes.⁶ These open metal- and ligand-terminated oligomers have been characterized by ¹H{³¹P}, ¹³C{¹H}, and ³¹P{¹H} NMR spectroscopy, MALDI-TOF MS, IR, UV-vis, and circular dichroism (CD) spectroscopies, elemental analysis, and size-exclusion chromatography (SEC). The length of **L**_{*m*}[**Pt**]_{*m*+1}Cl₂ can be determined on the basis of the ¹H methylene multiplet intensity ratio between the internal (~2.15 ppm) and terminal (~2.05 ppm) Pt(PEt₃)₂ groups as well as the ³¹P{¹H} intensity ratio between the internal (~13.3 ppm) and terminal (~16.6 ppm) PEt₃ groups. The length of **[Pt]**_{*n*}**L**_{*n*+1}H₂ can be similarly determined by the ¹H intensity ratio for the diagnostic 4,4'-protons of the binaphthyl units as well as the terminal alkyne protons. MALDI-TOF mass spectra showed the presence of molecular ion peaks for all the metal-terminated oligomers and ligand-terminated oligomers.

Treatment of metal-terminated **L**_{*m*}[**Pt**]_{*m*+1}Cl₂ with 1 equiv of ligand-terminated **[Pt]**_{*n*}**L**_{*n*+1}H₂ in the presence of CuCl catalyst at r.t. afforded cyclic species in very high total yields (Scheme 2). For example, by treating equimolar **L**[**Pt**]₂Cl₂ and **[Pt]**L₂H₂, molecular triangle (25%), hexagon (45%), and nonagon (15%) were efficiently assembled (with an overall yield of 85%). These chiral metallopolycycles were unambiguously characterized by MALDI-TOF MS and resulted from the [1 + 1], [2 + 2], and [3 + 3] cyclization processes, respectively.⁷ Metallopolycycles of much larger size have been synthesized by this process (Scheme 2). The largest metallopolycycle contains 47 [**Pt**] and 47 **L** units with a molecular weight of 39 847.5 Da. Molecular mechanics simulations indicated that the

Scheme 1



Scheme 2



reagents	products (yield %)			total yield (%)
	(<i>m</i> + <i>n</i> +1)	2(<i>m</i> + <i>n</i> +1)	3(<i>m</i> + <i>n</i> +1)	
<i>m</i> =1, <i>n</i> =1	3(25)	6(45)	9(15)	85
<i>m</i> =1, <i>n</i> =2	4(59)	8(20)	12(8)	87
<i>m</i> =1, <i>n</i> =3	5(77)	10(9)	15(2)	88
<i>m</i> =3, <i>n</i> =2	6(74)	12(15)	/	89
<i>m</i> =3, <i>n</i> =3	7(66)	14(9)	/	75
<i>m</i> =7, <i>n</i> =7	15(62)	30(7)	/	69
<i>m</i> =11, <i>n</i> =11	23(63)	/	/	63
<i>m</i> =15, <i>n</i> =15	31(57)	/	/	57
<i>m</i> =23, <i>n</i> =23	47(10)	/	/	10

internal cavities of these molecular polygons range from 0.9 to 22 nm.

The chiral molecular polygons have been characterized by ¹H{³¹P}, ¹³C{¹H}, and ³¹P{¹H} NMR spectroscopy, microanalysis, IR, UV-vis, and CD spectroscopies. In contrast to their open oligomeric starting materials, the NMR data of these chiral molecular polygons indicate a single ligand environment, suggesting the formation of cyclic species of *D*_{*n*} symmetry. As expected, the terminal C≡C-H stretches of **L-H**₂ at ~3300 cm⁻¹ disappear upon the formation of metallopolycycles. We have observed molecular ion peaks for all the metallopolycycles reported here in their MALDI-TOF mass spectra.

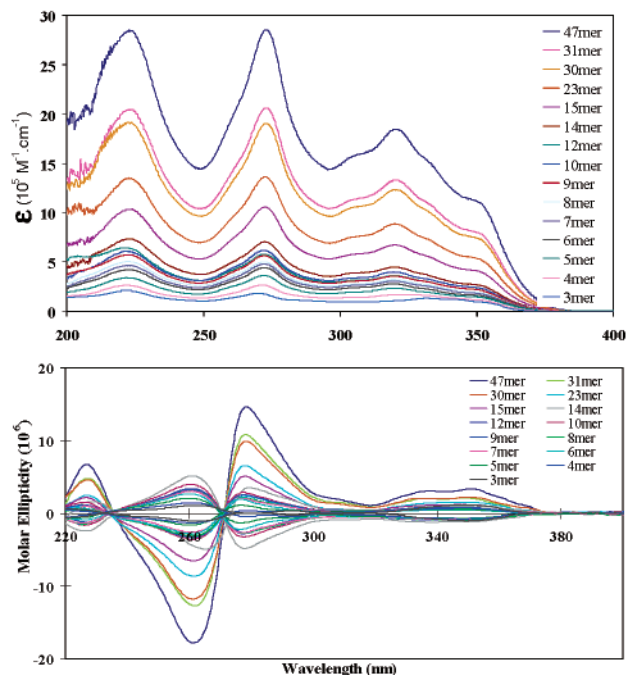


Figure 1. UV-vis (top) and CD (bottom) spectra of chiral metallocycles in an acetonitrile/dichloromethane mixture.

The electronic spectrum of $L-H_2$ shows two naphthyl $\pi \rightarrow \pi^*$ transitions at ~ 245 nm and three weak acetylenic $\pi \rightarrow \pi^*$ transitions at ~ 290 nm. Upon the formation of open oligomers and metallocycles, a new peak at ~ 220 nm appeared, assignable to the *trans*-Pt(PET₃)₂ moiety. The acetylenic $\pi \rightarrow \pi^*$ transitions red-shift and split into four peaks at ~ 303 , 318, 332, and 350 nm, a result of mixing of Pt p-orbitals into the acetylenic $\pi \rightarrow \pi^*$ bands.⁸ For $[Pt]_n L_{m+1} H_2$, there is still a $\pi \rightarrow \pi^*$ transition peak at ~ 245 nm due to the terminal naphthyl acetylene units. As expected, the extinction coefficients increase as the length of the open oligomers and the size of the metallocycles increase because of the presence of more *trans*-Pt(PET₃)₂ and **L** building units (Figure 1).

The open oligomers and metallocycles exhibit bisignate naphthyl $\pi \rightarrow \pi^*$ bands at ~ 260 and ~ 277 nm and acetylenic $\pi \rightarrow \pi^*$ signals at ~ 335 and ~ 352 nm. A new minor band also appears at ~ 226 nm for the metallocycles, which is assigned to the chiral arrangement of PET₃ groups. The CD signals increase steadily as the size of the metallocycle increases, consistent with an increasing number of *trans*-Pt(PET₃)₂ and **L** building units.

The mesoscopic nature of large polygons presents a significant challenge for their characterization. The identity of metal- and ligand-terminated oligomers has been unambiguously established on the basis of NMR data, microanalysis results, and MALDI-TOF MS. Although NMR and IR spectroscopic data and microanalysis results cannot differentiate metallocycles of different sizes, the presence of molecular ion peaks in the MALDI-TOF mass spectra of all the metallocycles unambiguously establishes their ring sizes. Furthermore, control experiments showed that a metal- or ligand-terminated open oligomer alone does not fragment under the conditions used for metallocycle synthesis; the metallocycles can thus only result from [1 + 1], [2 + 2], and [3 + 3] cyclization processes.⁶ This fact has enabled us to confirm the sizes of the metallocycles using SEC retention times. As shown in Figure 2, the plots of $\log(M_p)$ vs retention time can be linearly fitted for open oligomers and metallocycles. This linear dependence of $\log(M_p)$ on retention time indirectly proves the sizes of metallocycles. The

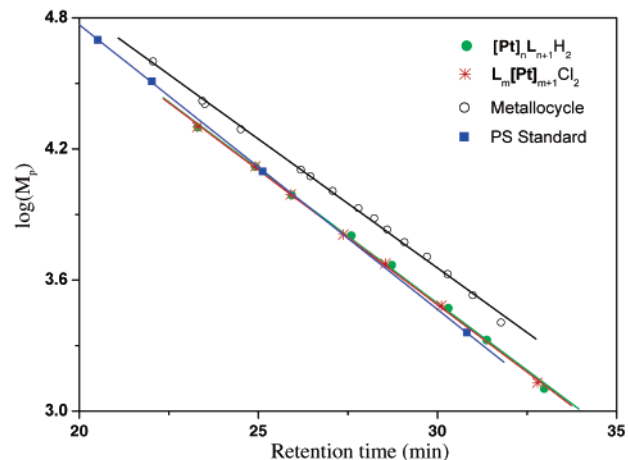


Figure 2. A plot of $\log(M_p)$ vs retention time for open oligomers and metallocycles in CH_2Cl_2 .

metal- and ligand-terminated oligomers fall essentially on the same line that matches well with that of polystyrene (PS) standards, thus confirming their formulation based on the spectroscopic data and microanalysis results. The lines for open oligomers have slightly larger slopes than that of PS standards, suggesting that open oligomers adopt more rigid structures than PS.⁹ The metallocycles on the other hand fall on a different line (with a larger slope) than the PS standard. On the basis of the SEC results, the metallocycles appear to have more compact and rigid structures than PS.

In summary, we have developed a facile approach toward nanoscopic and mesoscopic chiral molecular polygons. Such molecular polygons can be used as interesting building blocks for the construction of larger functional structures that cannot be accessed from a top-down approach.

Acknowledgment. We thank NSF (CHE-0208930) and ACS-PRF for financial support. W.L. is an A.P. Sloan Fellow, a Beckman Young Investigator, a Cottrell Scholar of Research Corp., and a Camille Dreyfus Teacher-Scholar.

Supporting Information Available: Experimental procedures, analytical data, 18 figures, and three tables. This material is available free of charge via the Internet at <http://pubs.acs.org>.

References

- (1) (a) Stang, P. J.; Olenyuk, B. *Acc. Chem. Res.* **1997**, *30*, 502–518. (b) Leininger, S.; Olenyuk, B.; Stang, P. J. *Chem. Rev.* **2000**, *100*, 853–907. (c) Fujita, M. *Chem. Soc. Rev.* **1998**, *27*, 417–425. (d) Holliday, B. J.; Mirkin, C. A. *Angew. Chem., Int. Ed.* **2001**, *40*, 2022–2043.
- (2) (a) Dinolfo, P. H.; Hupp, J. T. *Chem. Mater.* **2001**, *13*, 3113–3125. (b) Lee, S. J.; Lin, W. J. *Am. Chem. Soc.* **2002**, *124*, 4554–4555. (c) Lee, S. J.; Hu, A.; Lin, W. J. *Am. Chem. Soc.* **2002**, *124*, 12948–12949. (d) Merlau, M. L.; Mejia, M. D. P.; Nguyen, S. T.; Hupp, J. T. *Angew. Chem., Int. Ed.* **2001**, *40*, 4239–4242. (e) Cotton, F. A.; Lin, C.; Murillo, C. A. *Acc. Chem. Res.* **2001**, *34*, 759–771.
- (3) Jiang, H.; Lin, W. J. *Am. Chem. Soc.* **2003**, *125*, 8084–8085.
- (4) (a) Liu, Y.; Jiang, S.; Glusac, K.; Powell, D. H.; Anderson, D. F.; Schanze, K. S. *J. Am. Chem. Soc.* **2002**, *124*, 12412–12413. (b) Onitsuka, K.; Harada, Y.; Takei, F.; Takahashi, S. *Chem. Commun.* **1998**, 643–644.
- (5) A reagent ratio of 4:1 was used to minimize the formation of metallocycles.
- (6) $[Pt]_n L_{m+1} H_2$ should be formulated as $[Pt]_n L_{m-1} (L-H)_2$ except for $L-H_2$.
- (7) We proved this point by synthesizing triangle, hexagon, and nonagon with mixed methyl and acetyl protecting groups in 1:2 ratio. See Supporting Information.
- (8) Yam, V. W.-W. *Acc. Chem. Res.* **2002**, *35*, 555–563.
- (9) The slopes of the fitted lines for PS, metal- and ligand-terminated oligomers, and metallocycles are -0.130 , -0.123 , -0.122 , and -0.118 , respectively. A smaller slope indicates less drastic dependence of retention time on $\log(M_p)$ and thus suggests a less rigid structure.

JA049145M